

Clockwise vertical-axis rotation in the West Vardar zone of Serbia: Tectonic implications

Vesna Lesić, Emo Márton, Violeta Gajić, Dragana Jovanović, Vesna Cvetkov



Дигитални репозиторијум Рударско-геолошког факултета Универзитета у Београду

[ДР РГФ]

Clockwise vertical-axis rotation in the West Vardar zone of Serbia: Tectonic implications | Vesna Lesić, Emo Márton, Violeta Gajić, Dragana Jovanović, Vesna Cvetkov | Swiss Journal of Geosciences | 2018 | |

10.1007/s00015-018-0321-8

<http://dr.rgf.bg.ac.rs/s/repo/item/0003057>

Дигитални репозиторијум Рударско-геолошког факултета Универзитета у Београду омогућава приступ издањима Факултета и радовима запослених доступним у слободном приступу. - Претрага репозиторијума доступна је на www.dr.rgf.bg.ac.rs

The Digital repository of The University of Belgrade Faculty of Mining and Geology archives faculty publications available in open access, as well as the employees' publications. - The Repository is available at: www.dr.rgf.bg.ac.rs



Clockwise vertical-axis rotation in the West Vardar zone of Serbia: tectonic implications

Vesna Lesić¹ · Emő Márton²  · Violeta Gajić³ · Dragana Jovanović¹ · Vesna Cvetkov⁴

Received: 28 May 2018 / Accepted: 23 September 2018 / Published online: 24 October 2018
© Swiss Geological Society 2018

Abstract

The Vardar-Tethyan mega-suture between the Eurasian and Adria (Gondwana) margins comprises remnants of oceanic lithosphere of Neotethys and distal parts of the adjacent continental margins including unconformable Late Cretaceous sedimentary cover and Cenozoic igneous rocks of post-obduction age. This study provides kinematic constraints for displacements and rotations affecting the Serbian part of the West Vardar and Jadar-Kopaonik units after the closure of the Neotethyan (= Sava) Ocean. The targets of the paleomagnetic research were Late Cretaceous sediments representing an overstep sequence and a wide variety of Oligocene-Earliest Miocene igneous rocks. The studied 48 sampling points were distributed within two segments of a narrow and 160 km long strip of the Western Vardar zone, namely the wider Rudnik Mts. area to the north and the Kopaonik Mts. area to the south. The results of standard laboratory processing and statistical evaluation suggest that both studied segments of the Western Vardar zone were affected by 30°–46° clockwise vertical-axis rotation which must have taken place after 20 Ma. It is proposed that clockwise vertical-axis rotation documented in the present study on one hand, and the previously documented counterclockwise vertical-axis rotation of Adria, on the other hand are related to large scale extension in the southern Pannonian basin.

Keywords Paleomagnetism · Clockwise rotation · Dinarides · West Vardar zone

Editorial handling: K. Saric.

Electronic supplementary material The online version of this article (<https://doi.org/10.1007/s00015-018-0321-8>) contains supplementary material, which is available to authorized users.

✉ Vesna Lesić
vlesic@drenik.net

- ¹ Department of Geomagnetism and Aeronomy, Republic Geodetic Authority, Bul. Vojvode Mišića 39, Belgrade 11000, Serbia
- ² Paleomagnetic Laboratory, Mining and Geological Survey of Hungary, Columbus utca 17-23, Budapest 1145, Hungary
- ³ Department of Mineralogy, Crystallography, Petrology and Geochemistry, Faculty of Mining and Geology, University of Belgrade, Djušina 7, Belgrade 11000, Serbia
- ⁴ Department of Geophysics, Faculty of Mining and Geology, University of Belgrade, Djušina 7, Belgrade 11000, Serbia

1 Introduction

The Vardar zone as defined by Kossmat (1924) is a wide zone (Vardar-Tethyan mega-suture) that not only comprises remnants of oceanic lithosphere (obducted ophiolites and ophiolitic mélangé), but also distal parts of the ancient Gondwana margin (in the Serbian segment, the Drina–Ivanjica, the Jadar–Kopaonik units below the obducted West Vardar ophiolites, Fig. 1), and post-obduction sedimentary and igneous rocks. In the years to follow, the Vardar zone has been the subject of intensive geological studies and subdivided in different ways by different authors. Most recently Schmid et al. (2008) and Cvetković et al. (2016a) defined an ophiolitic zone named West Vardar ophiolites, which comprises the Vardar Zone Western Belt plus the Dinaric ophiolite belt sensu Karamata (2006) and a second zone, namely the Eastern Vardar ophiolites, equivalent to the Main Vardar Zone sensu Karamata (2006). Both ophiolite zones were obducted in the Latest Jurassic, i.e. before the suturing between Eurasia and Adria (= Gondwana). According to most authors, an oceanic realm between the two margins was still open in

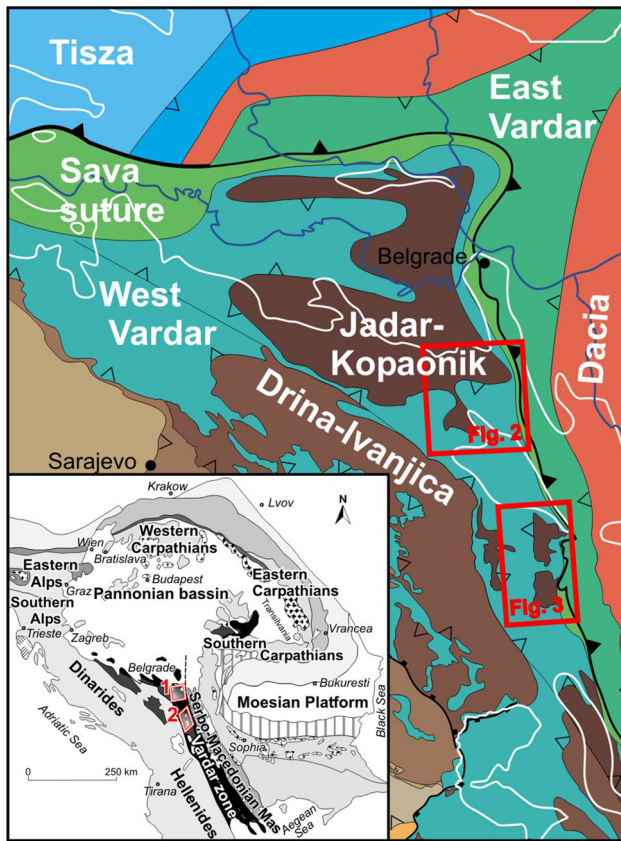


Fig. 1 The main geological units of the Vardar-Tethyan mega-suture (Cvetković et al. 2016a) and neighbouring areas after Schmid et al (2008). The following two study areas are marked by rectangles: The wide area of Rudnik Mts. (see Fig. 2) with Late Cretaceous and Oligocene-Miocene sampling localities/sites and the area of Kopaonik Mts. (Fig. 3) with Oligocene sampling localities/sites. The inset shows the place of the Vardar zone in the Carpatho-Balkan region with sampling areas indicated (red boxes)

the Cretaceous (Sava Ocean), but closed around the end of the Cretaceous-Paleocene boundary to form the Sava suture (Schmid et al. 2008; Cvetković et al. 2016a).

As mentioned above, the ancient Gondwana margin that became obducted by the West Vardar ophiolites is represented by the Adriatic microplate. The Cenozoic rotation of this microplate with respect to Africa was in a counter-clockwise (CCW) sense but timing and duration of the decoupling process are still a matter of discussion (Márton 2006; Ustaszewski et al. 2008; Márton et al. 2011; van Hinsbergen et al. 2014; Márton et al. 2017a). The representative of the stable European margin on the European side of the Vardar zone, the Moesian platform (inset of Fig. 1) did not rotate during the Cenozoic (van Hinsbergen et al. 2008). However, so far no reliable paleomagnetic results were available for the area between these two differently behaving, relatively rigid areas to constrain possible rotations which could have affected the Vardar zone en block or different parts of it in different ways.

This paleomagnetic study focuses on Upper Cretaceous sediments and Oligocene to Miocene magmatic rocks from two areas within the area of the Jadar-Kopaonik unit and the West Vardar ophiolites located immediately west of the Sava suture (Fig. 1). The sampled Upper Cretaceous lithologies formed during the closure of the Sava Ocean, while the formation of the Cenozoic lithologies post-dated collision between Adria and Europe (Cvetković et al. 2016a). The older substratum on which the Cretaceous and younger sediments were deposited, or became intruded by magmatic rocks, is assigned to different tectonic units, comprising ophiolites and continental assemblages (see Figs. 1, 2, 3) and was probably affected by later differential

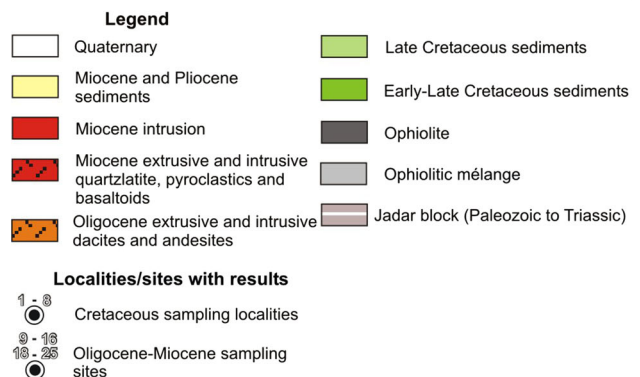
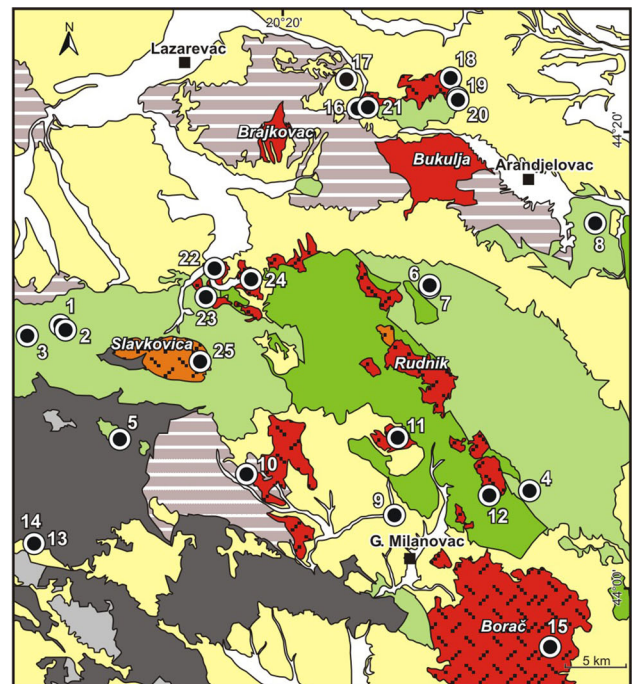


Fig. 2 Simplified geological map of the wider area of the Rudnik Mts. (see location in Fig. 1) based on the Basic Geological Maps of Former Yugoslavia (Federal Geologic Survey Belgrade, scale 1:100,000) covered by sheets Gornji Milanovac, Kragujevac, Kraljevo, Smederevo, Obrenovac and Čačak with sampling localities. The paleomagnetic localities/sites are numbered and referred to in the text and in Tables 1 and 2

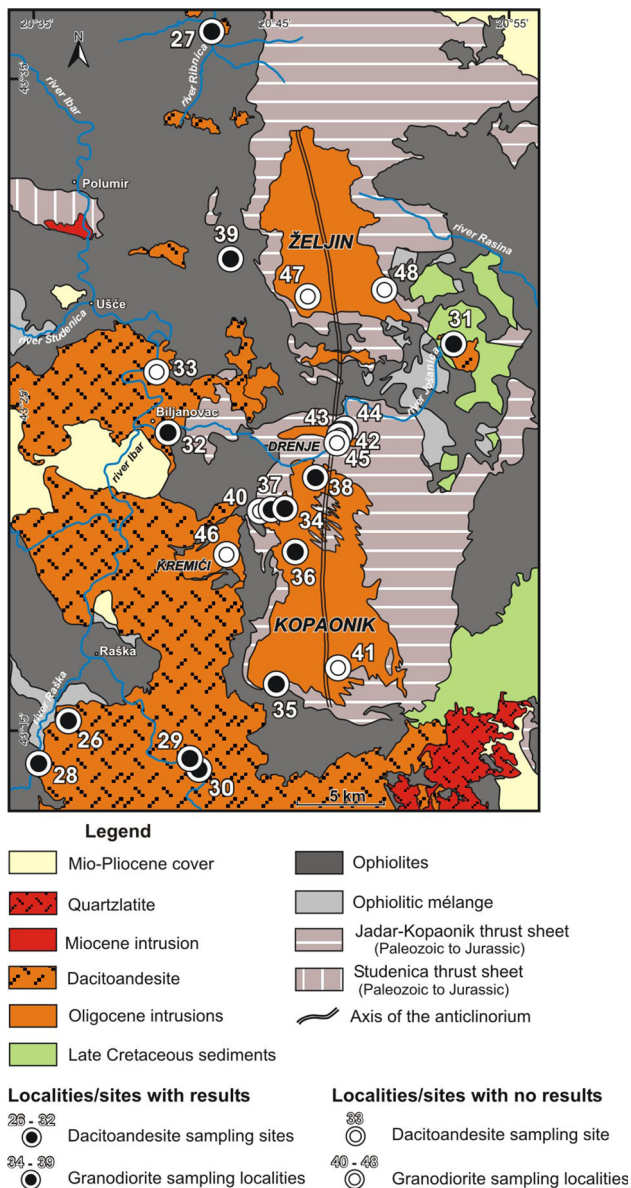


Fig. 3 Simplified geological map of the Kopaonik Mts. area (see location in Fig. 1) based on Geological Maps of Former Yugoslavia (Federal Geologic Survey Belgrade, scale 1:100,000) covered by sheets Vrnjci and Novi Pazar with sampling localities. The paleomagnetic localities/sites are numbered and referred to in the text, in Table 3 and Supplementary Table 1

vertical-axis rotations, as can be suspected by looking at the non-linear shape of the Sava suture, especially in the area north of Belgrade (Fig. 1).

2 Geological background

The Serbian part of the Vardar–Tethyan mega-suture is dominated by ophiolites, but also comprises Gondwana (Jadar–Kopaonik and Drina–Ivanjica units) and Eurasia (Tisza and Dacia Mega-units) derived continental blocks

(Fig. 1). The mega-suture is subdivided into several sub-units, which are defined and named differently by different authors based on different geotectonic concepts. It is beyond the scope of this paper to discuss these differences in detail, but we will briefly outline some of them. Dimitrijević (1997) distinguishes three subzones: (1) the External Vardar subzone, comprising the Srem, Jadar, and Kopaonik blocks, (2) the Central Vardar subzone and (3) the Internal Vardar subzone. Karamata et al. (1999) and Karamata (2006), following a terrane concept, define a Western Vardar zone that docked with the Jadar block at the end of the Cretaceous, and the main Vardar zone. Between these two zones he defined the Kopaonik Block and Ridge unit. Schmid et al. (2008) distinguishes a Western and an Eastern Ophiolite belt, and between the two the Sava suture (see Gawlick et al. 2017 for a comparison between the different subdivisions).

Almost all of the localities/sites sampled by us belong to the Western Vardar zone, Jadar block and Kopaonik Block and Ridge unit sensu Karamata (2006), or in other words to the West Vardar and Jadar–Kopaonik units sensu Schmid et al. (2008). Only a single locality (Cretaceous limestone at locality No. 8, see Fig. 2) is located in the East Vardar unit.

The early geological and tectonic history of the Vardar zone is not of direct interest for the interpretation of our results, therefore only a few important events will be highlighted. These are: (1) rifting stage and formation of ophiolites starting in the Late Anisian, (2) obduction of the West Vardar ophiolites over Adria-derived units (e.g. the Jadar–Kopaonik unit) in the Latest Jurassic–Earliest Cretaceous (Gawlick et al. 2017 and references therein), (3) sedimentation of shallow, followed by deeper water carbonates and flysch onto the ophiolites and/or the Jadar–Kopaonik unit, starting in the Cretaceous and ending at around the Cretaceous–Paleogene boundary (Schmid et al. 2008). After the final closing of the Sava suture, different tectono-magmatic conditions led to widespread magmatism and formation of continental sedimentary basins (Cvetković et al. 2016a).

The targets of this study are limestones and marls (Turonian–Maastrichtian) as well as clastic carbonate turbidites (Campanian–Maastrichtian), representing an overstep sequence, deposited on continental slopes (Gajić 2014), a variety of Eocene–Early Miocene magmatic rocks from the wider Rudnik Mts. area (Fig. 2), and Oligocene I-type granitoids and dacitoandesites from the Kopaonik Mts. area (Fig. 3; Schefer et al. 2011).

According to the Basic Geological Maps of Former Yugoslavia (scale 1:100 000, sheets: Gornji Milanovac, Filipović et al. 1976; Kragujevac, Brković et al. 1979; Kraljevo, Marković et al. 1967; Smederevo, Pavlović et al. 1979; Obrenovac, Filipović et al. 1979 and Čačak, Brković et al. 1977) covering the wider area of the Rudnik Mts. (Fig. 2) the oldest outcropping rocks belonging to the Jadar

Table 1 Wider Rudnik Mts. area, Cretaceous sediments

Locality	Lat. N Lon. E	Lithology	n/no	D°	I°	k	α_{95}°	D_c°	I_c°	k	α_{95}°	dip	Age
1 Struganik upper quarry 4241–262	44°11'13" 20°06'53"	Limestones white, greyish white and red	9/22	211.8	– 49.1	156	4.1	212.3	– 45.2	156	4.1	39/4	Upper Campanian-Lower Maastrichtian
2 Struganik lower quarry 4263–272	44°11'25" 20°06'17"	Limestones greyish	10/10	222.2	– 49.7	60	6.3	209.3	– 49.1	60	6.3	309/11	Upper Campanian-Lower Maastrichtian
3 Breždje 4299–313	44°10'57" 20°04'14"	Marly limestones greyish-white	14/15	230.3	– 39.4	78	4.5	219.7	– 32.6	78	4.5	340/16	Santonian
4 Vračevšnica 4314–325	44°04'22" 20°34'50"	Flysch grey	6/12	218.9	– 40.3	328	3.7	237.7	– 15.5	328	3.7	94/50 99/41	Upper Cenomanian-Turonian
5 Gajić quarry 4283–298	44°06'26" 20°09'59"	Limestone pinkish grey	15/16	38.8	47.4	211	2.6	36.2	26.7	211	2.6	28/21	Santonian-Campanian
6 Bogdanović quarry 3955–977, 4045–057 4114–137	44°13'15" 20°28'41"	White limestone red limestone	18/61 30/61	260.8	– 52.7	59	4.5	251.7	– 48.5	62	4.4	Variable	Upper Campanian
7 Tolić quarry 4015–022	44°13'14" 20°28'43"	Limestone Red	8/8	359.9*	58.0*	271	3.4	350.1	46.2	271	3.4	322/14	Upper Campanian
8 Lipovica quarry 4201–225	44°16'05" 20°39'05"	Limestone variegated	16/25	5.8*	52.7*	39	6.0	36.0	50.6	34	6.4	Variable	Turonian

Summary of locality mean paleomagnetic directions based on the results of principal component analysis (Kirschvink 1980). Key: Lat. N and Lon. E: geographic coordinates (WGS84), n/no: number of used/collected samples; D , I (D_c , I_c): declination, inclination before (after) tilt correction; k and α_{95} : statistical parameters (Fisher 1953). The paleomagnetic directions, considered in tectonic interpretation are in bold

Remarks: Locality 1: samples left out are most likely the re-deposited shallow water carbonates with negative susceptibility either scattered directions or bad demagnetization curves. *Left out from tectonic interpretation due to closeness to the direction of present Earth magnetic field on the sampling area. Magnetic readings for the field orientation of the cores were corrected using IGRF-12 International Geomagnetic Reference Field model (Thébaud et al. 2015). The age determination was done by Milena Dunić based on well preserved microfossil associations except for localities 4 and 8 where the age is from the Basic Geological Map of former Yugoslavia

Table 2 Wider Rudnik Mts. area, Oligocene-Miocene sites

	Locality	Lat. N Lon. E	Lithology	n/no	D°	I°	k	α_{95}°	Age (K/Ar)
9	Šilopaj 3223-229	44°03'15" 20°26'39"	Basalt	5/6	60.1	52.9	94	7.9	25.71 ± 1.24 Ma
10	Ozrem 3205-213	44°05'00" 20°17'41"	Basaltic trachyandesite	7/9	179.3	- 64.4	173	4.7	24.87 ± 0.95 Ma 35 ± 0.95 Ma
11	Mutanj 3214-222	44°06'39" 20°26'43"	Rhyodacite	9/9	174.0	- 33.9	211	3.8	
12	Beli kamen 3230-249	44°04'09" 20°32'22"	Leucominette	19/19	207.3	- 49.0	16	8.7	24.1 ± 0.93 Ma
13	Družetić 1 3192-198	44°01'52" 20°04'48"	Basalt	7/7	28.9	48.1	294	3.5	23.9 ± 2.1 Ma
14	Družetić 2 3199-204	44°01'52" 20°04'48"	Basalt	6/6	39.2	56.9	145	5.6	
15	Borač 3365-372	43°57'34" 20°36'07"	Quartz latite	7/8	13.5	66.8	215	4.1	23-20 Ma
16	Kruševica quarry 3729-738	44°21'04" 20°24'15"	Quartz latite	10/10	210.8	- 59.3	73	5.7	25.56 ± 1.20 Ma
17	Čik quarry - Karačevac 3748-755	44°22'21" 20°23'34"	Quartz latite	6/8	64.1	79.1	43	10.4	
18	Kremštak 3768-785	44°22'27" 20°29'53"	Porouse quartz latite	13/18	64.0	56.3	30	7.7	
19	Čirić quarry 3786-804	44°21'36" 20°30'19"	Porouse quartz latite	16/19	96.5	39.7	119	3.4	26.67 ± 1.04 Ma
20	Žuti Oglavak 4089-099	44°21'33" 20°30'22"	Porouse quartz latite	11/11	97.8	40.9	75	5.3	26.62 ± 1.60 Ma
21	Bukačina stena 3739-747	44°21'04" 20°24'53"	Ignimbrite	9/9	314.5	47.6	251	3.3	25.16 ± 0.89 Ma
22	Miljakovac quarry 3917-926	44°14'00" 20°15'37"	Ignimbrite	10/10	32.9	50.0	571	2.0	
23	Bela stena 3927-936	44°12'44" 20°15'06"	Ignimbrite	10/10	55.8	62.7	154	3.9	
24	Poljanice 4226-240	44°13'31" 20°17'50"	Ignimbrite	13/15	10.1	34.0	168	3.2	
25	Slavkovica 3353-364	44°09'55" 20°14'46"	Dacite	12/12	207.6	- 45.5	421	2.1	32 Ma

Summary of site mean paleomagnetic directions based on the results of principal component analysis (Kirschvink 1980). Key: Lat. N and Lon. E: geographic coordinates (WGS84), n/no: number of used/collected samples; D, I: declination, inclination; k and α_{95} : statistical parameters (Fisher 1953)

Remark for ages: Ages for sites 9, 10, 12, 13, 14 and 15 published in Cvetković et al. (2013) and ages for the rest are from personal communication with Cvetković

block are Paleozoic to Jurassic very low grade metamorphic and/or silicified/dolomitized sediments. They are overlain by Jurassic ophiolitic mélangé and obducted ophiolites. After an erosional event, a Cretaceous sedimentation cycle started at various times, depending on the location. This produced Aptian flysch and younger (clastic, carbonate and marly) sediments, and terminated with the deposition of flysch during the Campanian-Maastrichtian

(Toljic et al. 2018). The Upper Cretaceous sediments are subdivided into four lithostratigraphic units (Gajić 2014): (1) basal coarse-grain clastites of Albian-Cenomanian and Cenomanian age, (2) Cenomanian and Lower Turonian clastic-carbonate rocks from the shelf, (3) Turonian to Maastrichtian limestones and marls with cherts deposited on the continental slope, (4) clastic-carbonate turbidites of Campanian-Maastrichtian age.

Table 3 Kopaonik Mts. area, Oligocene sites (26–32) and localities (34–39)

	Locality	Lat. N Lon. E	Lithology	n/no	D°	I°	k	α_{95}°
26	Velika Bisina 3667–683	43°15'17" 20°36'13"	Dacitoandesite	17/17	174.8	– 30.6	86	3.9
27	Kamenica 3652–666	43°36'33" 20°42'4"	Dacitoandesite	14/15	203.4	– 15.4	70	4.8
28	Panojevići 3684–695	43°13'58" 20°34'54"	Dacitoandesite	12/12	223.4	– 60.5	212	3.0
29	Rudnica 1 3640–651 3640–651	43°13'60" 20°41'28"	Dacitoandesite	11/12	239.1	– 42.3	162	3.6
30	Rudnica 2 3696–707	43°13'57" 20°41'34"	Dacitoandesite	12/12	238.0	– 40.9	84	4.8
31	Ploče 3630–639	43°26'56" 20°52'24"	Dacitoandesite	10/10	234.2	– 61.0	88	5.2
32	Biljanovac 3645–560	43°24'02" 20°40'31"	Dacitoandesite	12/16	218.3	– 24.7	102	4.3
34	Kokorovo 3344–352	43°21'51" 20°45'20"	Granodiorite	9/9	12.8	18.0	68	6.3
35	Lisina 3407–415	43°16'24" 20°44'57"	Granodiorite	9/9	27.1	23.3	221	3.5
36	Gvozdac 3416–421	43°20'31" 20°45'48"	Granodiorite	6/6	33.0	48.5	17	16.9*
37	Samokovska reka 3394–406	43°21'51" 20°44'48"	Granodiorite	9/13	17.3	22.0	57	6.9
38	Šutanovina 3533–544	43°22'44" 20°46'37"	Granodiorite	6/12	45.8	35.7	60	8.9
39	Dubovo 3523–532, 3523–532	43°29'30" 20°43'03"	Granodiorite	8/10	17.9	37.1	37	9.3

Summary of mean paleomagnetic directions based on the results of principal component analysis (Kirschvink 1980). Key as for Table 2. The granodiorites are 30.6–31.7 Ma old while the age of the dacitoandesites is 31 Ma

Remark: *Locality 36 is omitted from the compilation of the overall mean palaeomagnetic direction due to α_{95} exceeding 16° . Sites/localities yielding no meaningful palaeomagnetic result are summarized in Supplementary Table 1

The Miocene (Oligocene) magmatic rocks intrude into, or overlie, mainly Cretaceous sediments. According to their age (Cvetković and Pécskay 1999; Prelević et al. 2000; Jovanović 2003; Cvetković et al. 2004, 2007, 2013, 2016b; Prelević et al. 2005) they can be divided in three groups (for details see chapter „Paleomagnetic sampling“). The Neogene infill within the research area is represented by fresh water and brackish sediments, conglomerate, marls, marls with intercalation of tuffs, clays, sandstones and marly limestone.

The oldest outcropping rocks in the wider area of Kopaonik Mts. are Late Palaeozoic to Early Jurassic low-grade metamorphic sediments (Basic Geological Maps of Former Yugoslavia, scale 1:100,000, sheets: Vrnjci and Novi Pazar, Urošević et al. 1973a, b). They are part of the Jadar–Kopaonik unit and can be subdivided into a western

(Studenica) and eastern (Kopaonik) thrust sheet (Fig. 3). These thrust sheets are tectonically overlain by ophiolitic mélange of Middle (?)–Late Jurassic age and obducted Jurassic ophiolites of the West Vardar unit (Dimitrijević 1997; Schmid et al. 2008; Schefer et al. 2011). The Kopaonik thrust sheet forms an anticlinorium with undulating N–S axis (Urošević et al. 1973a, b), which is intruded by I-type granitoids (e.g. Kopaonik, Drenje, Željina and Kremići, Fig. 3; Schefer et al. 2011). In the Željina pluton and more prominently, in the Drenje massif, enclaves of more mafic composition are common. East of the Željina–Kopaonik anticlinorium weakly metamorphosed Senonian flysch with large olistoliths unconformably overlies the metamorphic series and/or the obducted ophiolites (e.g. Schefer et al. 2011). Dacitoandesites and volcanoclastic rocks are mostly known from the Ibar Valley located west of the Kopaonik

pluton. They either intrude or overlie ophiolites. Also, small dacitoandesite bodies are exposed on the eastern side of the Kopaonik pluton where they intrude post-Turonian sediments and serpentinite. In the Ibar Valley, near Polumir, an S-type two-mica leucocratic schistose granite intrudes the Studenica thrust sheet. SE of the Kopaonik pluton volcanics of quartzlatite composition does occur.

The I-type granodiorites were dated as Oligocene, the S-type granite as Miocene in age (U–Pb method, 30.6–31.7 Ma and 18.1–17.4 Ma, respectively, Schefer et al. 2011). The dacitoandesites were considered to be older than the granodiorite intrusions since the Kremiči intrusion caused metamorphic/metasomatic changes in the surrounding dacitoandesites (Mičić 1980), or alternatively, partly synchronous with the Kopaonik intrusion (Dimitrijević 1997). The isotope ages for the dacitoandesite extrusions and volcanoclastic rocks confirm the latter view (Cvetković et al. 1995).

3 Paleomagnetic sampling

The paleomagnetic samples were drilled in the field with a portable gasoline powered motor drill. All were oriented with a magnetic compass, the igneous samples also with a sun compass. The geographic coordinates were measured by GPS (Garmin GPSmap 60CSx).

From the wider Rudnik Mts. area (Fig. 2), limestones/marls (7 localities, 157 independently oriented samples) and flysch (one locality, 12 independently oriented samples) of Upper Cretaceous age were collected, most of them from quarries. Four of the quarries were of special interest for the following reasons. Amongst two quarries located close to each other near Bosuta (localities 6 and 7), one only exposed dark red micritic limestone (Folk 1959, 1962), while in the other one some strata were dark red, others whitish. Moreover some beds exhibited concentric features varying both in size and colours on the surface, with the continuation of colour variation downward in the bed. We drilled the concentric features of varying colours and, as we shall see later, the analysis of their natural remanent magnetization provided a key to the correct interpretation of the relative ages of the remanence connected to the red and whitish limestones, respectively. A second pair of localities near Struganik (1 and 2) exposed two types of limestones containing cherts. One is an autochthonous micritic limestone (Folk 1959, 1962) which is the indigenous rock (whitish, greyish colour) deposited in a pelagic environment. It contains an Upper Campanian-Lower Maastrichtian globotruncanid association (Gajić 2007, 2014). The second type is a shallow marine allochemsparite limestone (Folk 1959, 1962) (red or white) deposited from turbidity flows. We drilled a fairly

large number of samples from both types. The Oligocene-Miocene igneous rocks of different compositions were sampled at 17 sites (187 independently oriented samples), some very close to the Cretaceous localities (Fig. 2). The first suite (K/Ar age is 32–29 Ma) consists of extrusive and shallow intrusive dacite and andesite (locality 25). The second suite is of Latest Oligocene-Early Miocene age (K/Ar age: 26–19 Ma). It consists of extrusive and shallow intrusive quartzlatite (localities 15–20), quartzlatite–rhyodacite pyroclastics (localities 21–24), basaltoids that mostly occur as several meter thick dykes and sills or lava plugs, rarely as lava flows (localities 9–14), and finally I-type granitoids. The third suite comprises Early-Middle Miocene S-type granites (K/Ar age: 20–17 Ma) which are not the subjects of this study.

In the area of Kopaonik Mts. (Fig. 3) Oligocene dacitoandesites were sampled at eight localities (104 independently oriented cores). Oligocene I type granodiorite of the Kopaonik and related plutons, were drilled at 15 localities (167 independently oriented cores). The Kopaonik pluton is built up from different types of intrusive igneous rocks and has a zonal distribution. The central part is of porphyritic quartz monzonite and granite. In the southwest porphyritic granodiorite is found, while in the north normal grained granodiorite prevails grading into fine-grained granodiorite and quartz diorite toward the margin. Along the northwest margin endomorphically altered diorite occurs. We drilled mostly the marginal parts of the pluton because in the central part (higher altitudes) the granodiorite occurred as huge loose blocks transported over different distances due to glaciation and gravity (Urošević et al. 1973a, b).

4 Laboratory processing

One, or when long enough, several standard - size specimens were cut from the cores of one inch diameter. Then the NRM was measured in the natural state using JR-5 and JR-5A magnetometers (AGICO, Brno). This was followed by anisotropy of magnetic susceptibility (AMS) measurements with KLY-2 or with MFK1-A kappabridges with Jelínek (1977) method. The computer programs used for measurements and evaluations were Aniso (Bohrás 1990) and ANISOFT 4.2 and 5.1 (Chadima and Jelínek 2008; Chadima et al. 2018) based on Jelínek (1978, 1981).

Test samples from each group were demagnetized in increments with alternating field (AF) (AFD300, Magnon, Dassel and LDA-3A, AGICO) or with the thermal (MMTD80, Magnetic Measurements, Aughton, and TSD-1, Schonstedt Instrument Company, Reston) method. The remaining samples from the respective groups were demagnetized with the more efficient method, and in as

many steps as was necessary, to define the components of the NRM.

In order to control the magnetic mineralogy, Curie-points were determined on selected samples from the igneous rocks (KLY-2 combined with CS-1 or CS-3 both from AGICO). Lowrie-experiments (Lowrie 1990) were made on the sediments and on some igneous rocks (using MMPM10 magnetizer, Magnetic Measurements).

The above laboratory experiments were carried out in the Paleomagnetic laboratory of the Mining and Geological Survey of Hungary and Paleomagnetic laboratory of the Republic Geodetic Authority of Serbia.

5 Results

In the following chapter the obtained results will be presented according to the measured lithologies.

5.1 Upper Cretaceous sediments, wider Rudnik Mts. area

The limestones/marls were of different colours, whitish grey, yellowish white, pinkish, red or variegated. In the red samples from the concentric feature from locality 6, the magnetic mineral was invariably hematite (e.g. Fig. 4,

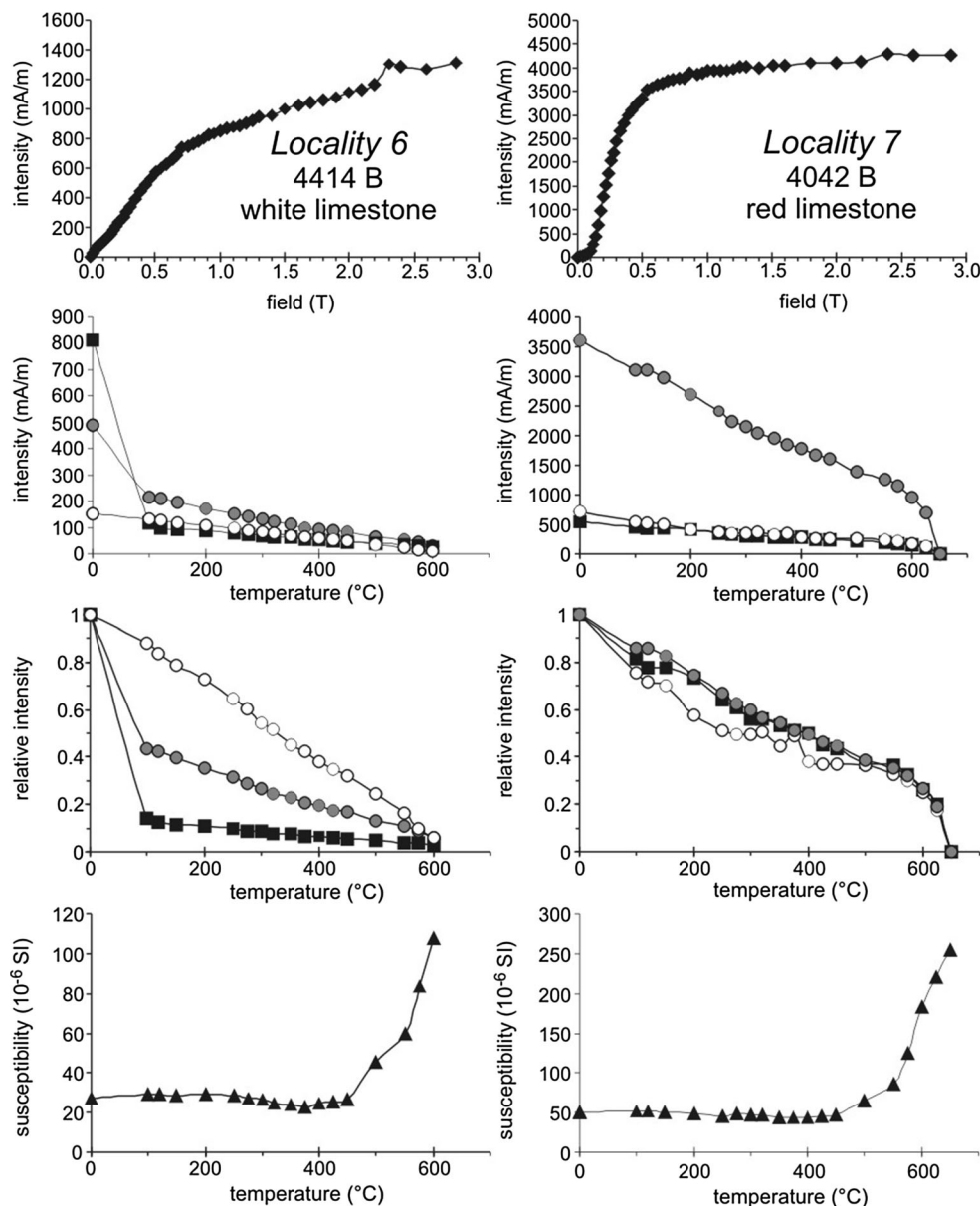


Fig. 4 Data from the Cretaceous sediments of the wider Rudnik Mts. area regarding the identification of magnetic minerals (method by Lowrie 1990). From top to bottom: IRM acquisition, thermal demagnetization of the three-component IRM and its normalized

version, susceptibility during heating. The components of the IRM were acquired in fields of 2.8 T (squares), 0.8 T (full circles) and 0.12 T (open circles)

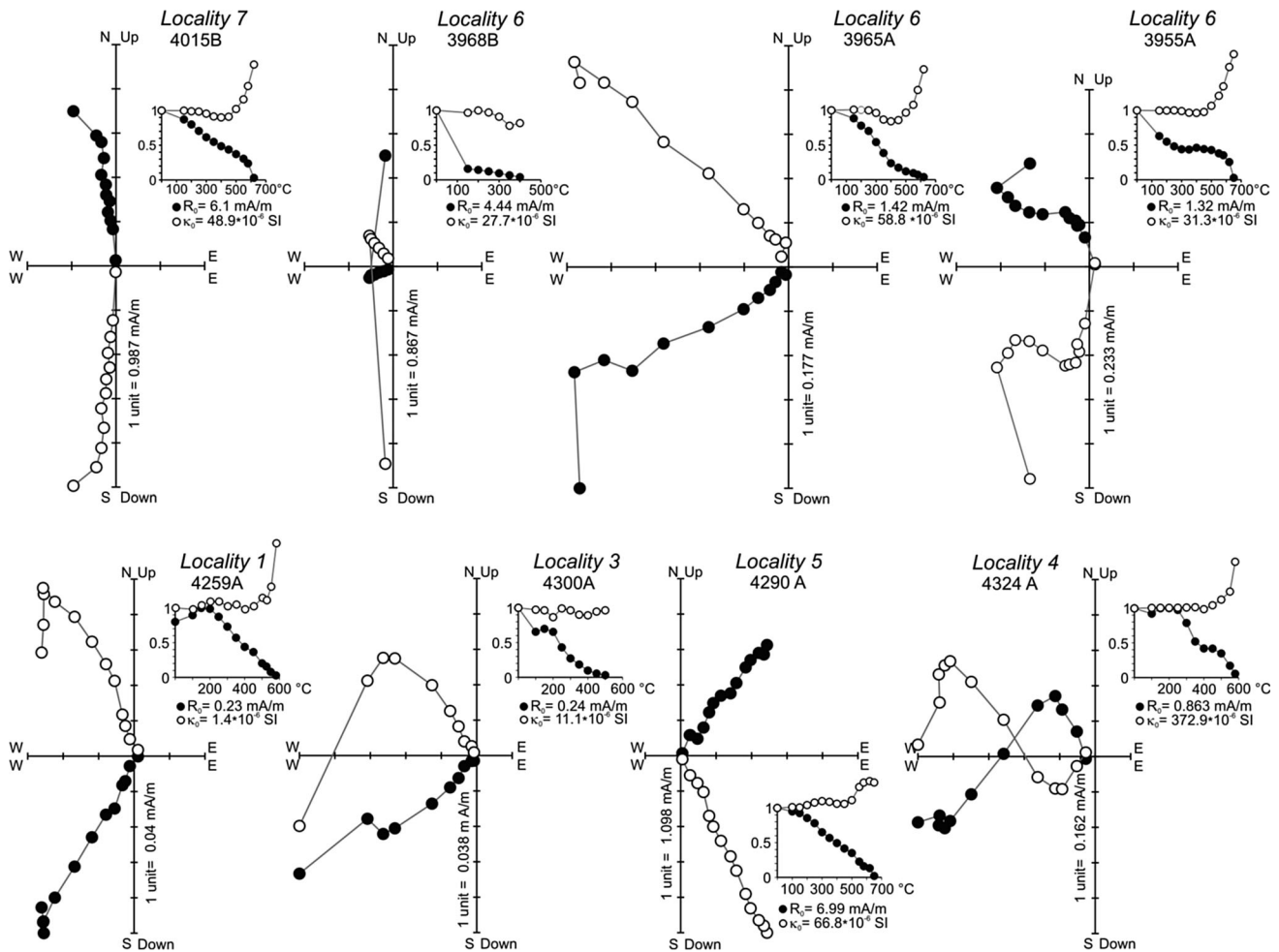


Fig. 5 Typical demagnetization curves for the Cretaceous sediments of the wider Rudnik Mts. area. Key for the Zijderveld diagrams: projection of the NRM vector into the horizontal (black dots) and into

the vertical (open circles), for the normalized intensity/susceptibility versus temperature diagrams: open circles: susceptibility, dots: intensity

specimen 4042B). In the whitish grey samples magnetite was accompanied by goethite (e.g. Fig. 4, specimen 4114B). As the bed with the concentric feature had an alteration of whitish and red cylinders, and the latter always contained hematite which was magnetized in the present Earth magnetic field, while the whitish ones had an „ancient“ component (see below), we could conclude that the beds of red colour were not deposited in a more oxygenated environment than the less abundant white beds.

The magnetic fabrics of the Cretaceous sediments are typical for undeformed sediments. The degree of AMS is low (locality mean P values are between 1.016–1.046), foliation is bedding parallel, the maximum and intermediate susceptibility axes are intermixed (Supplementary Fig. 1). This suggests that the sediments were not seriously deformed after the crystallization of the magnetic minerals.

The characteristic remanence for all the sampled sediments was isolated with stepwise thermal demagnetization and component analysis. It was found that red and

variegated samples typically had single component NRMs, aligned with or close to the direction of the present Earth magnetic field at the sampling area (Fig. 5, specimen 4015B). In these samples the carrier of the characteristic remanence was hematite (Table 1, items marked with stars). The white parts of the cylindrical features at locality 6 and the whitish-greyish samples in general exhibited practically single component magnetization, departing in a clockwise (CW) sense from the present north (Fig. 5, specimens 3968B, 3965A, 4259A, 4290A). The yellowish white and pinkish carbonate samples and the flysch had complex NRM, but the overprint and the ancient components were separable. Either the overprint was easily removable and the component decaying towards the origin was regarded as ancient, or, as in specimens 3955A, 4324A (Fig. 5, yellowish-white carbonate and flysch), the component interpreted as ancient was „surrounded“ by an easily removable overprint and one with higher unblocking

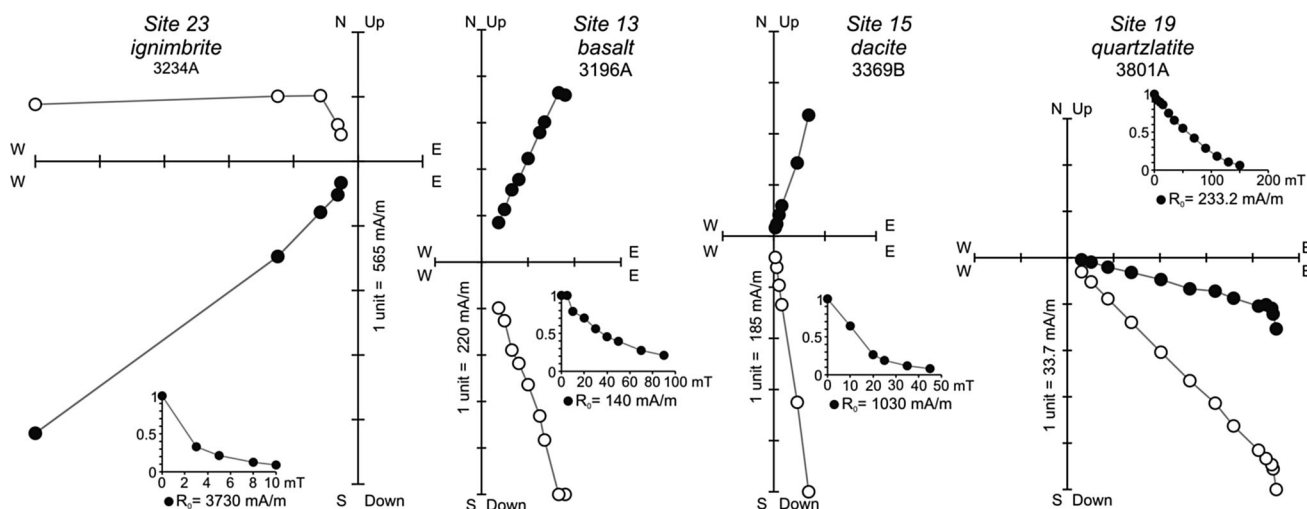


Fig. 6 Typical demagnetization curves for different lithologies of Oligocene-Miocene igneous sites from the wider Rudnik Mts. area. Key as for Fig. 5, but in case of AF demagnetization the intensity versus AF field is plotted

temperature with orientation similar to the removed overprint.

5.2 Oligocene-Earliest Miocene magmatic rocks, wider Rudnik Mts. area

Among the igneous rocks from the wider Rudnik Mts. area (Fig. 2) there are basalts, andesites, rhyodacites, quartzlatites and ignimbrites of quartzlatitic composition. Curie-point measurements identified magnetite (Supplementary Fig. 2) and the magnetic softness of the NRM (Fig. 6) corroborated that the carrier of the remanence was indeed a magnetite-type mineral in the studied rocks, irrespective of the great variety in composition.

The AMS was measured for all sites. The degree of anisotropy varied between 1.014 and 1.046 for most of them, higher values were only observed for sites 12 and 16 (1.095 and 1.125, respectively). The orientations of the principal susceptibility axes are random for sites 9–12 and 15. Concerning the rest, there is a variation from poorly to tightly grouped types (Supplementary Fig. 3), but foliation degree (F) is always higher than lineation (L). The inclinations of the poles of foliation vary between 11° and 69°.

The NRM was efficiently demagnetized with AF method (Fig. 6). The sites mean paleomagnetic directions, some of them with normal, others with reversed polarity, are characterized by excellent or good statistical parameters (Table 2).

5.3 Oligocene magmatic rocks, wider Kopaonik Mts. area

The NRM in the granodiorites resides in magnetite, as Curie-point measurements prove (Lesić et al. 2013). In

contrast, there is a wide variation of the magnetic minerals in the dacitoandesites. The Curie-point measurement on specimen 3651 from site 29 (Supplementary Fig. 4) shows an increase of susceptibility upon heating from room temperature to about 250 °C, a minimum at about 350 °C and above that a magnetite phase (somewhat oxidized?). In the cooling curve the first phase is not detectable. This can be interpreted as evidencing the oxidation of Ti-magnetite to titanomaghemite, which converts to hematite (Moskowitz 1981 cited in Collinson 1983) at 350 °C, causing a drop in susceptibility and the absence of the first phase on cooling. Note that the susceptibility monitored during stepwise thermal demagnetization behaves in a similar manner (Fig. 7, specimen 3651A). On the other hand hematite must be mentioned, which is the only carrier of the NRM at locality 32 (see Lowrie experiment, Lesić et al. 2013).

The results of the AMS measurements carried out on the same samples as those used for the paleomagnetic processing, including their interpretation, were published earlier for the dacito-andesites as well as the granodiorites (Lesić et al. 2013). In this paper they will be discussed later and in the context with their possible influence on the paleomagnetic vectors.

The Oligocene dacito-andesites from the Kopaonik Mts. area (Fig. 3) were thermally demagnetized. The NRM decayed to the Curie point of the magnetite (Fig. 7), except for site 32, where the magnetic mineral, according to the demagnetization curve (Fig. 7, specimen 3548B) of the NRM as well as the magnetic mineralogy experiment (Lesić et al. 2013) is hematite. In contrast to the dacitoandesites, most granodiorites were unsuitable to provide stable NRM. Nevertheless, samples from a number of

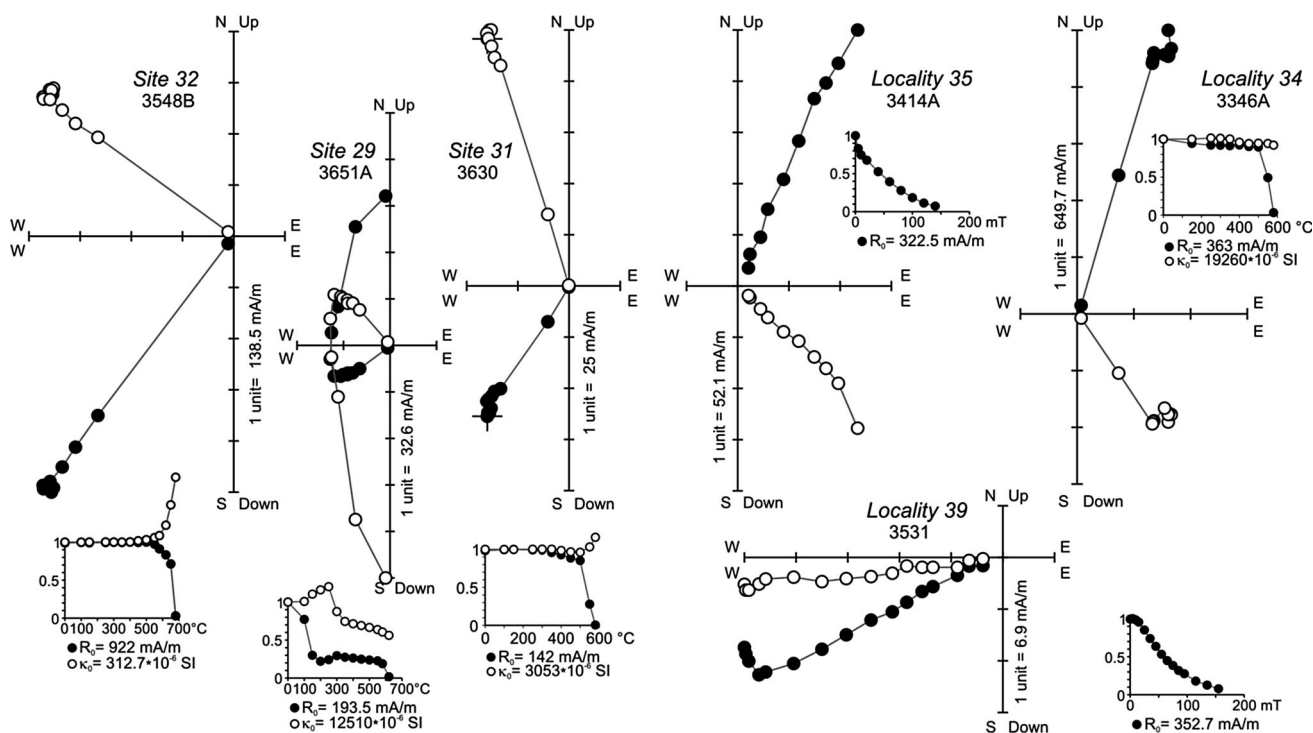


Fig. 7 Typical demagnetization curves of Oligocene dacitoandesites (sites 32, 29, 31) and granodiorites (localities 35, 34, 39) from the Kopaonik Mts. area. For key see Fig. 5

localities provided excellent demagnetization curves, responding well to both thermal and AF methods (Fig. 7).

6 Discussion

All the sampled Upper Cretaceous localities exhibit statistically well-defined characteristic remanence; k values are between 39 and 328, confidence angles well below 10° (Table 1). However, results from localities 7 and 8 and that of the red samples from locality 6 must be excluded from tectonic interpretation, due to closeness to the direction of the present Earth magnetic field in the sampling area and the secondary origin of the carrier of the remanence, which is hematite. The secondary origin of the hematite is documented by sedimentological and paleontological investigations, which identified iron sulphide inside the chambers of the microfossils in the whitish limestone at locality 6, a primary mineral, which must have been oxidized to hematite in the dark red strata. The same mechanism could have produced hematite also in other Upper Cretaceous limestones of red or variegated colours.

The rest of the results shown in Table 1 exhibit paleomagnetic directions, which significantly depart from the direction of the present Earth magnetic field at the sampling area before tilt corrections. The between-locality reversal test (McFadden and McElhinny 1990) is positive

(Table 4). These features characterize „ancient“ magnetizations, which are not necessarily primary, but were acquired while the tectonic unit remained in the same orientation at the same latitude. The more powerful tilt test (Enkin 2003) points to the post-tilting age of the remanence (Fig. 8).

It follows from the above reasoning that the paleomagnetic direction of tectonic significance should be computed from the locality mean directions before tilt corrections (bold in Table 1). Five of them exhibit a tight cluster; locality 6 seems to be an outlier. While we have no direct evidence for the presence of hematite (carrying present overprint) in the white specimens from locality 6 (Fig. 4, specimen 4414B and Fig. 5, specimen 3968B), even a tiny un-removed component residing in the possibly present tiny hematite flakes can somewhat distort the component attached to magnetite. This could justify omitting the results departing from the cluster, a procedure that would not really modify the overall mean direction, but considerably improve its statistical parameters (Table 4).

The characteristic remanent magnetizations for the Oligocene-Earliest Miocene igneous rocks from the wider Rudnik Mts. area are also excellent from a statistical point of view. The whole population of the site mean directions exhibits Fisherian distribution. Most of the sites mean directions are well-grouped, but some considerably depart from the cluster (Fig. 9). The overall mean paleomagnetic

Table 4 The overall mean directions for the Cretaceous, Oligocene-Miocene and Oligocene localities/sites from the wider Rudnik Mts. and Kopaonik Mts. areas

	N	D°	I°	k	α_{95}°	Tilt-test optimal untilting	Rev. Class.	VGP			
								Lat.N°	Long.E°	K	A95°
Wider Rudnik area, Cretaceous, localities 1–6, post-tilting remanence	6	46.3	47.4	41.7	10.5	9.4% (± 31.6)	Rbi	50.2	116.8	27.1	13.1
Wider Rudnik area, Cretaceous, localities 1–5, post-tilting remanence	5	40.7	45.3	139.1	6.5	4.8% (± 61.2)	Rai	53.4	124.4	126.7	6.8
Wider Rudnik area, Oligocene-Miocene, sites 9–25	17	34.3	57.9	10.8	11.4		Rc				
Wider Rudnik area, Oligocene-Miocene, without sites 11, 19–21	13	33.0	57.2	27.2	8.1		Rb	64.6	109.5	16.7	10.5
Wider Kopaonik area, Oligocene, sites/localities 26–32, 34–35, 37–39	12	30.5	35.7	13.6	12.2		Rc	55.5	140.5	13.8	12.1

Key: N: number of localities/sites; D, I: declination, inclination; k, α_{95}° and K, A95° statistical parameters (Fisher 1953) of the paleomagnetic directions and virtual geomagnetic poles, respectively; Rev.Class: classification of reversal test (McFadden and McElhinney 1990); VGP: Virtual Geomagnetic Pole; Lat. N, Long. E: latitude and longitude of the Virtual Geomagnetic Pole, respectively. The tilt-test (Enkin 2003) is negative for the Cretaceous sediments

direction was calculated in two versions. One based on 17, the other on 13 sites (Table 4). Omitting sites, which considerably (40° or more, a limit set by Wilson et al. 1972) depart from the overall mean paleomagnetic direction has little influence on the direction itself, yet improves considerably the statistical parameters. The outliers could have been affected by moderate post-emplacement tilting, though we have no field evidence for this. Emplacement during the excursions of the Earth magnetic field cannot be excluded, either.

The igneous rocks of Oligocene age from the Kopaonik Mts. area, dacitoandesites and granodiorites, also suggest CW rotation with respect to the present north (Fig. 10 and Table 4). The population shows Fisherian distribution, the reversal test is positive. It is, however, remarkable that the overall mean inclination is shallower than that for the Rudnik Mts. area. Inclination flattening due to magnetic anisotropy could account for the flattening in the granodiorites (AMS degree varies between 1.06–1.61 for the localities yielding statistically well-defined paleomagnetic

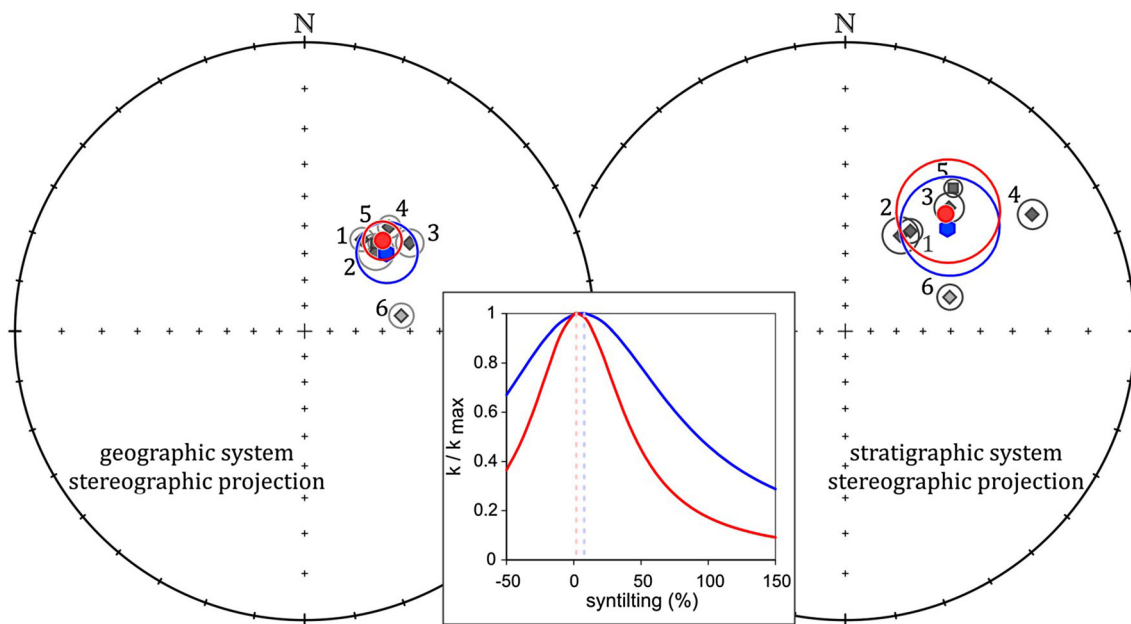


Fig. 8 Regional tilt test for Cretaceous sediments from the wider Rudnik Mts. area. Locality mean directions are given with α_{95} (grey symbols). Square: normal polarity; diamonds: originally reversed polarities. Blue hexagon and red dot with α_{95} are the overall mean

directions calculated for localities 1–6 and 1–5 respectively. The middle diagram shows stepwise back-tilting (blue, all localities, red, locality 6 is omitted). The tilt-test (Enkin 2003) is negative

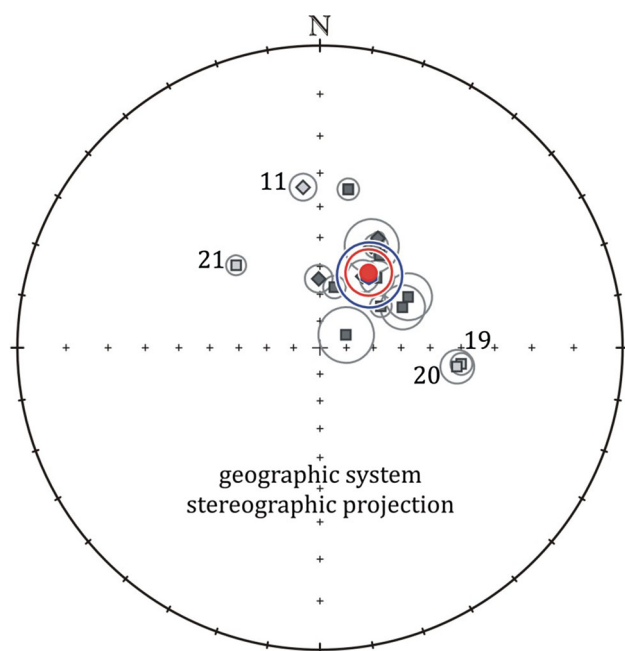


Fig. 9 Site mean paleomagnetic directions (grey squares and diamonds) with α_{95} for Oligocene-Miocene igneous rocks from the wider Rudnik Mts. area. Reversed paleomagnetic directions are shown as normal polarities (diamonds). Overall mean directions with α_{95} were calculated for all sites (blue) and without 11, 19–21 (in red), respectively

directions). However, shallow inclinations also occur among the dacitoandesites (e.g. 27 and 32, Fig. 10), which have weak anisotropies (max. 1.05, Lesić et al. 2013). So far we cannot point out a feasible mechanism for the shallow inclinations since bias due to overprinting is unlikely (the demagnetization curves of the NRM's are very simple, Fig. 7).

The overall mean paleomagnetic directions (Table 4) for the Cretaceous and Oligocene to Earliest Miocene localities/sites from the wider Rudnik Mts. area, as well as those for the Oligocene localities from the Kopaonik Mts. area are interpreted to indicate CW vertical-axis rotations with respect to the present north (Fig. 11). In the case of the Rudnik Mts. area the overall mean directions calculated from the locality or site mean paleomagnetic directions of the Upper Cretaceous sediments suggest $46.3^\circ \pm 15.5^\circ$. The Oligocene-Earliest Miocene igneous rocks yielded $34.3^\circ \pm 20.3^\circ$ CW vertical-axis rotation (data are based on 6 localities and 17 sites, respectively). The error of the rotation angle is that of the mean declination. Since the overall mean paleomagnetic directions of the Cretaceous sediments (which are of post-tilting age) and those for the Oligocene-Earliest Miocene igneous rocks are very close in the Rudnik Mts. area (Table 4), we conclude that the former became re-magnetized during the volcanic activity and the rotation must have taken place after 20 Ma, which is

the upper age limit (Table 2) for the studied igneous rocks from the wider Rudnik Mts. area.

The overall mean paleomagnetic direction for the Kopaonik Mts. area suggests a post-Oligocene CW vertical-axis rotation of $30.3^\circ \pm 15.0^\circ$. Considering the estimated error angle of rotations we suggest that a more or less uniform vertical-axis rotation affected both areas, hence an about 160 km long and presently NNW-SSE oriented part of the Vardar-Tethyan mega-suture, which also includes the adjacent Sava suture.

The long and relatively narrow shape of the studied belt (Fig. 1) naturally raises the question if the above rotations can be related to deformations within the belt, since there is ample evidence for post-Oligocene deformation events there (Schefer et al. 2011; Mladenović et al. 2015). The answer is no, for the change in the orientation of the stress or strain field, where applicable, would need rotation in the opposite sense. Therefore it is more likely that the studied areas belong to a larger unit which underwent CW vertical-axis rotation as opposed to CCW rotated Adria. A number of not yet published and partly preliminary paleomagnetic results from the Timok magmatic complex (Lesić et al. 2017), from the area S of Belgrade (Šumadija, Márton et al. 2017b), from the Danubicum (Lesić et al. 2015; Panaiotu et al. 2012), all located further east from the area of the present study (Fig. 12), point to the feasibility of such an interpretation. However, the degree of co-ordination of the

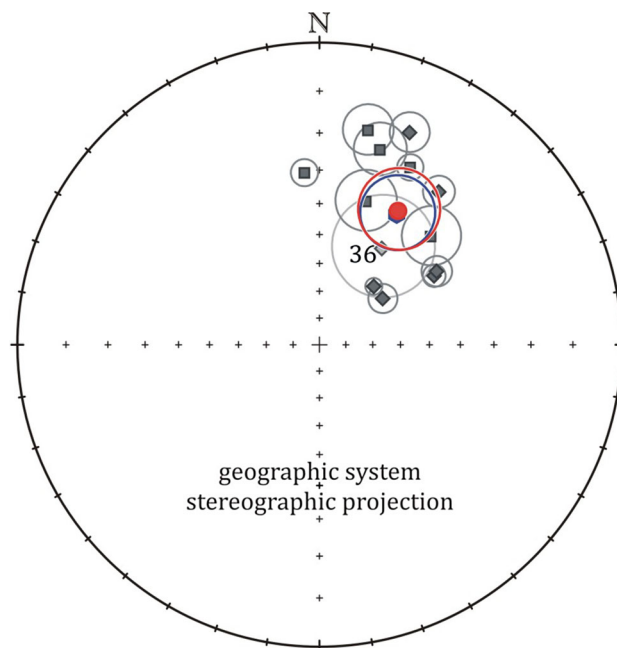


Fig. 10 Site mean paleomagnetic directions for the Kopaonik Mts. area (squares are for the granodiorites, all normal polarities, diamonds are for dacitoandesites, all reversed polarities) with α_{95} . The reversed paleomagnetic directions are shown as normal. Overall mean direction with α_{95} , all sites/localities (blue), without locality 36 (red)

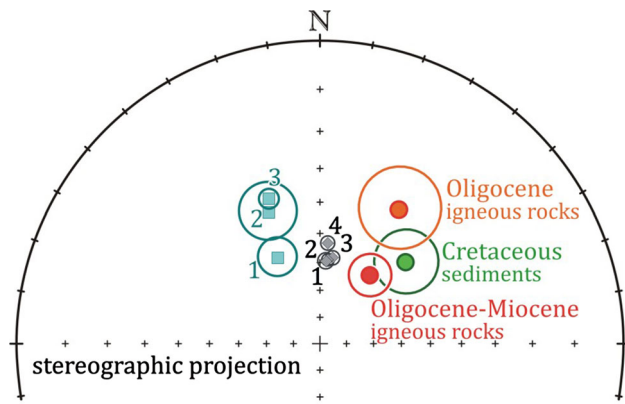


Fig. 11 Comparison of the overall mean paleomagnetic directions of the present study with those expected for a reference location 43.7°N, 20.7°E of the study area from Adria poles (1–3 in blue) for 41, 52 and 75 Ma (Márton et al. 2017a). For the same reference location, the expected directions from stable Europe poles (1–4 in grey) are for 20, 30, 40 and 70 Ma, respectively (Torsvik et al. 2012)

region affected by CW rotation is a question that remains open. The same applies to the boundary between CCW rotated stable Adria (Márton 2006; Márton et al. 2017a), and the CW rotated part of the Vardar zone.

Interestingly, a CCW rotation of Adria and a CW rotation of the studied sector „Rudnik-Kopaonik strip“ including the Timok area was predicted by a kinematic retrodeformation by Ustaszewski et al. (2008; their Fig. 6). This retrodeformation only took into account deformations and rotations during the past 20 Ma and did not consider paleomagnetically deduced large-scale rotations as input; it was solely based on estimates of Miocene compression (Alps and Carpathians) and extension (Pannonian basin) in the Alps-Carpathians-Dinarides system. According the cited study this differential rotation is clearly related to the opening of the Pannonian basin. Matenco and Radivojević (2012; their Fig. 12) performed a study of intensive Miocene extension in the Serbian part of the Pannonian basin and concluded that this extension is the result of a combination of slab rollback in the Carpathians and the retreating slab beneath the external Dinarides. The results of our study are in line with these interpretations. Most importantly, they quantify the amount of clockwise rotation of the part of the Vardar-Tethyan mega-suture located south of Belgrade and turn out to be larger than the 16°, estimated by Ustaszewski et al. (2008).

Earlier published paleomagnetic studies (Lesić et al. 2007; Cvetkov et al. 2012) were carried out in Fruška Gora (Fig. 12). This inselberg in the South Pannonian basin is built up by basement that also contains ophiolites of West Vardar affinity (Toljić et al. 2012) and Mesozoic cover, which feature an E–W oriented antiform, surrounded and partly covered by Miocene sediments of the Pannonian basin. According to Schmid et al. (2008), Fruška Gora

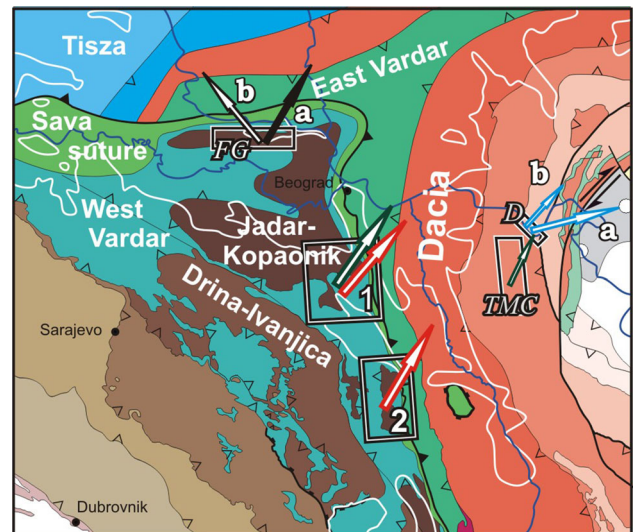


Fig. 12 The main geological units of the Vardar-Tethyan mega-suture (Cvetković et al. 2016a) and neighbouring areas after Schmid et al. (2008). Arrows (long: final, short: preliminary results) indicate the overall-mean paleodeclinations. The study areas are marked by rectangles. Key: 1—wider Rudnik Mts. area, 2—wider Kopaonik Mts. area, FG—Fruška Gora, TMC—Timok Magmatic Complex, D—Danubicum. Age constraints for the rotations are as follows: post-Early Miocene for area 1 (this study); post-Oligocene for area 2 (this study); post-Oligocene to pre-Middle Miocene for area FG a; post-Middle Miocene to pre-Pliocene for area FG b (data for FG are from Lesić et al. 2007 and from Cvetkov et al. 2012); post-Late Cretaceous for area TMC (Lesić et al. 2017); post-Late Jurassic for area D (a after Panaiotu et al. 2012 and b after Lesić et al. 2015)

belongs to the Sava zone, which turns from a NNW-SSE strike south of Belgrade to a W-E orientation W of Belgrade.

A set of the paleomagnetic results from Fruška Gora represented the Oligocene latites and thermally affected Cretaceous flysch, north of the Fruška Gora antiform (Lesić et al. 2007; Cvetkov et al. 2012), while a single site of Oligocene andesite came from the area south of the same area (Cvetkov et al. 2012). They exhibited about 30° CW vertical-axis rotation, after correcting for the general northward tilting of the Fruška Gora during the Miocene. The 30° CW was followed by about 40° CCW vertical-axis rotation just before the Latest Miocene. The age of the CW rotation is constrained by the Oligocene age of the latites and the Middle Miocene age of the covering sediments, already exhibiting CCW rotation. Assuming that the latter is manifested in the dramatic change of the orientation of the Sava zone, north of Belgrade (which at more or less the same time suffered 30°–40° CW rotation in the Vardar-Tethyan mega-suture south of Belgrade), we can rely on the model of Toljić et al. (2012) who account for the 70° vertical-axis CW rotation as being due to large scale extensional deformation terminating before Mid-Miocene.

7 Conclusions

1. Upper Cretaceous sediments and extrusive magmatic rocks from the wider Rudnik Mts. area comprising West Vardar and Jadar-Kopaonik units of the Vardar-Tethyan mega-suture, yield regionally consistent paleomagnetic directions indicating 34°–46° CW vertical-axis rotation. This rotation took place after 20 Ma.
2. Further south, in the Kopaonik Mts. area, intrusive and extrusive igneous rocks of Oligocene age from the West Vardar and Jadar–Kopaonik units exhibit about 30° CW vertical-axis rotation.
3. Considering the statistical error accompanying the overall mean paleomagnetic directions, the rotations for the above mentioned groups are considered as being uniform.
4. The CW rotations documented by this study affected a narrow belt that is 160 km long. Although the area was internally deformed in several phases during the Miocene and later the changes in the orientation of the stress/strain field cannot be the consequence of the observed rotations.
5. Unpublished and partly preliminary paleomagnetic results from the Danubian nappes and from the Timok magmatic complex (both belonging to the Carpatho-Balkanides) and from Šumadija, S of Belgrade (E Vardar and Sava zones) also document CW vertical-axis rotations. This suggests that the narrow belt analysed by the present study is part of a larger region affected by CW rotation. However, this can only be confirmed after the so far unpublished results are finalized.
6. The CW vertical-axis rotation documented in the present study on the one hand, and the CCW vertical-axis rotation of Adria, on the other hand, go hand in hand with large scale extension documented for the southern Pannonian basin.

Acknowledgements We thank Milena Dunčić for age determinations of sediment samples. We also thank Nada Vasković and Dragan Milovanović for guiding us in the field and Vladica Cvetković for the discussions concerning the petrology and geochemistry of the studied areas. We gratefully acknowledge Stefan Schmid for his highly constructive review for the first and the present version of the manuscript. Also, helpful review by an anonymous referee is gratefully acknowledged. This work was supported by the Ministry of Science and Education of Serbia (Project No. 176016) and by the Hungarian Scientific Research Fund OKTA K105245.

References

Bodrás, R., (1990) Aniso – anisotropy program package for IBM PC. ELGI, Budapest

- Brković, T., Malešević, M., Klisić, M., Urošević, M., Trifunović, S., Radovanović, Z., et al. (1977). *Basic Geological Map of SFRJ, sheet Čačak (scale 1:100 000)*. Beograd: Savezni Geološki Zavod.
- Brković, T., Radovanović, Z., & Pavlović, Z. (1979). *Basic Geological Map of SFRJ, sheet Kragujevac (scale 1:100 000)*. Beograd: Savezni Geološki Zavod.
- Chadima, M., Hrouda, F., Jelínek, V. (2018). Anisoft 5.1—Advanced treatment of magnetic anisotropy data. *Geophysical Research Abstracts* 20, EGU-2018-15017.
- Chadima, M., & Jelínek, V. (2008). Anisoft 4.2.—Anisotropy data browser. *Contributions to Geophysics and Geodesy*, 38, 41.
- Collinson, D. W. (1983). *Methods in rock magnetism and palaeomagnetism, techniques and instrumentation* (p. 503). London: Chapman and Hall.
- Cvetkov, V., Lesić, V., & Vasković, N. (2012). New paleomagnetic results for Tertiary magmatic rocks of Fruška Gora, Serbia. *Annales géologiques de la Peninsule Balkanique*, 73, 99–108.
- Cvetković, V., Karamata, S., Knežević-Đorđević, V. (1995). Volcanic rock of the Kopaonik area. [Savetovanje “Geologija i metalogenija Kopaonika”]. *Republički društveni fond za geološka istraživanja Srbije, 19–22 jun 1995*, 185–195 (in Serbian with English abstract).
- Cvetković, V., & Pécskay, Z. (1999). The Early Miocene eruptive complex of Borač (central Serbia): Volcanic facies and evolution over time. Extended abstract. *Carpathian Geology* 2000, October 11–14, 1999, Smolenice. *Geologica Carpathica*, 50, 91–93.
- Cvetković, V., Pécskay, Z., & Šarić, K. (2013). Cenozoic igneous tectonomagmatic events in the Serbian part of the Balkan Peninsula: inferences from K/Ar geochronology. *Geologia Acta Vulcanologica*, 25, 111–120.
- Cvetković, V., Poli, G., Christofides, G., Koroneos, A., Pécskay, Z., Resimić-Šarić, K., et al. (2007). The Miocene granitoid rocks of Mt. Bukulja (central Serbia): Evidence for Pannonian extension-related granitoid magmatism in the northern Dinarides. *European Journal of Mineralogy*, 19(4), 513–532.
- Cvetković, V., Prelević, D., Downes, H., Jovanović, M., Vaselli, O., & Pécskay, Z. (2004). Origin and geodynamic significance of Tertiary post-collisional basaltic magmatism in Serbia (central Balkan Peninsula). *Lithos*, 73(3–4), 161–186.
- Cvetković, V., Prelević, D., Schmid, S. (2016a). Geology of South Eastern Europe. In P. Papić (Ed.) *Mineral and Thermal Waters of Southeastern Europe. Environmental Earth Sciences*. https://doi.org/10.1007/978-3-319-25379-4_1
- Cvetković, V., Šarić, K., Pécskay, Z., & Gerdes, A. (2016b). The Rudnik Mts. volcano-intrusive complex (Central Serbia): An example of how magmatism controls metallogeny. *Geologia Croatica*, 69, 89–99.
- Dimitrijević, M. D. (1997). *Geology of Yugoslavia* (p. 187). Beograd: Geoinstitut-Barex.
- Enkin, R. (2003). The direction-correction tilt test: An all-purpose tilt/fold test for paleomagnetic studies. *Earth and Planetary Science Letters*, 212, 151–166.
- Filipović, I., Pavlović, Z., Marković, B., Rodin, V., Marković, O., Gagić, N., et al. (1976). *Basic Geological Map of SFRJ, sheet Gornji Milanovac (scale 1:100 000)*. Beograd: Savezni Geološki Zavod.
- Filipović, I., Rodin, V., Pavlović, Z., Marković, B., Milićević, M., & Atin, B. (1979). *Basic Geological Map of SFRJ, sheet Obrenovac (scale 1:100 000)*. Beograd: Savezni Geološki Zavod.
- Fisher, R. (1953). Dispersion on a sphere. *Proceedings of the Royal Society of London Series A*, 217, 295–305.
- Folk, R. L. (1959). Practical petrographic classification of limestones. *American Association of Petroleum Geologists Bulletin*, 43, 1–38.

- Folk, R. L. (1962). Spectral subdivision of limestone types. In W. E. Ham (Ed.), *Classification of carbonate Rocks-A Symposium: American Association of Petroleum Geologists Memoir 1* (pp. 62–84). Berlin: Springer.
- Gajić, V. (2007). Petrology of Upper Cretaceous sedimentary rocks in the area Planinica-Struganik (Western Serbia). MSc thesis, University of Belgrade, Faculty of Mining and Geology, Belgrade, Serbia, 108 pp. (in Serbian).
- Gajić, V. (2014). Sedimentology of Upper Cretaceous of the central part of the Vardar zone. Ph.D. dissertation, University of Belgrade, Faculty of Mining and Geology, Belgrade, Serbia, 265 pp. (in Serbian).
- Gawlick, H. J., Sudar, M. N., Missoni, S., Suzuki, H., Lein, R., & Jovanović, D. (2017). Triassic-Jurassic geodynamic history of the Dinaric Ophiolite Belt (Inner Dinarides, SW Serbia). *Journal of Alpine Geology*, 55, 1–167.
- Jelínek, V. (1977). *The statistical theory of measuring anisotropy of magnetic susceptibility of rocks and its application*. Brno: Geofyzika s.p.
- Jelínek, V. (1978). Statistical processing of anisotropy of magnetic susceptibility measured on groups of sediments. *Studia Geophys Geodynamics*, 22, 50–62.
- Jelínek, V. (1981). Characterization of magnetic fabric of rocks. *Tectonophysics*, 79, T63–T67.
- Jovanović, M.M. (2003). Tertiary basaltic rocks in Serbia. *PhD thesis*, University of Belgrade, Faculty of Mining and Geology, Belgrade, Serbia, 299 pp. (in Serbian).
- Karamata, S. (2006). The geological development of the Balkan Peninsula related to the approach, collision and compression of Gondwana and Eurasian units. In A.H.F. Robertson & D. Mountrakis (Eds.), *Tectonic development of the Eastern Mediterranean region* (pp. 155–178). Geological Society London, Special. Publication, 260.
- Karamata, S., Dimitrijević, N. M., & Dimitrijević, D. M. (1999). Oceanic realms in the central part of the Balkan Peninsula during the Mesozoic. *Geologica Carpathica, special issues*, 50, 151–153.
- Kirschvink, J. L. (1980). The least-squares line and plane and the analysis of paleomagnetic data. *Geophysical Journal of the Royal Astronomical Society*, 62, 699–718.
- Kossmat, F. (1924). Geologie der zentralen Balkanhalbinsel, mit einer Übersicht des dinarischen Gebirgsbaus. In J. Wilder (Ed.), *Die Kriegsschauplätze 1914–1918 geologisch dargestellt* (p. 198). Berlin: Verlag Gebrüder Bornträger.
- Lesić, V., Márton, E., Cvetkov, V. (2007). Paleomagnetic detection of Tertiary rotations in the Southern Pannonian Basin (Fruška Gora). *Geologica Carpathica*, 58, 185–193.
- Lesić, V., Márton, E., Cvetkov, V., Gajić, V., Jovanović, D. (2017). Western Vardar zone, Danubicum and Timok magmatic complex (Serbia): Cordinated or independent CW rotation. *EGU series: Émile Argand Conference - 13th Workshop on Alpine Geological Studies, Abstract volume, Serbia*, pp 58.
- Lesić, V., Márton, E., Cvetkov, V., & Tomić, D. (2013). Magnetic anisotropy of Cenozoic igneous rocks from the Vardar zone (Kopaonik area, Serbia). *Geophysical Journal International*, 193, 1182–1197.
- Lesić, V., Márton, E., Cvetkov, V., Tomić, D. (2015). Paleomagnetic evidence for post-collisional Miocene clockwise rotation in the Serbian segment of the Vardar Zone and the Danubicum. *26th IUGG General Assembly, Prague, Abstracts*, IUGG-1324.
- Lowrie, W. (1990). Identification of ferromagnetic minerals in a rock by coercitive and unblocking temperature properties. *Geophysical Research Letters*, 17, 159–162.
- Marković, B., Pavlović, Z., Terzin, V., Urošević, M., Antonijević, R., Milosavljević, M., et al. (1967). *Basic Geological Map of SFRJ, sheet Kraljevo (scale 1:100 000)*. Beograd: Savezni Geološki Zavod.
- Márton, E. (2006). Paleomagnetic evidence for Tertiary counter-clockwise rotation of Adria with respect to Africa. In N. Pinter, Gy. Grencsics, J. Weber, S. Stein, D. Medak (Eds.), *The Adria microplate: GPS Geodesy, Tectonics and Hazards*, (pp 71–80). NATO Science Series IV – 61.
- Márton, E., Toljić, M., Lesić, M., Cvetkov, V., Stojadinović, U., Jovanović, D. (2017b) Paleomagnetically indicated rotations in the Sava zone and in the active European continental margin, Belgrade area. *EGU series: Émile Argand Conference - 13th Workshop on Alpine Geological Studies, Abstract volume, Serbia*, pp 66.
- Márton, E., Zampieri, D., Čosović, V., Moro, A., & Drobne, K. (2017a). Apparent polar wander for Adria extended by new Jurassic paleomagnetic results from stable core: Tectonic implications. *Tectonophysics*, 700–701, 1–18.
- Márton, E., Zampieri, D., Kázmér, M., Dunkl, I., & Frisch, W. (2011). New Paleocene-Eocene paleomagnetic results from the foreland of the Southern Alps confirm decoupling of stable Adria from the African plate. *Tectonophysics*, 504, 89–99.
- Matenco, L., & Radivojević, D. (2012). On the formation and evolution of the Pannonian Basin: Constrains derived from the structure of the junction area between the Carpathians and Dinarides. *Tectonics*, 31, TC6007. <https://doi.org/10.1029/2012tc003206>.
- McFadden, P. L., & McElhinney, M. W. (1990). Classification of the reversal test in palaeomagnetism. *Geophysical Journal International*, 103, 725–729.
- Mičić, I. (1980). *Contact, pneumatolytic and hydrothermal alterations in igneous rocks of Kopaonik region*. Memories du service geologique et geofisique, Vol. XIX, 1-138, Beograd.
- Mladenović, A., Trivić, B., & Cvetković, V. (2015). How tectonics controlled post-collisional magmatism within the Dinarides: Inferences based on study of tectono-magmatic events in the Kopaonik Mts. (Southern Serbia). *Tectonophysics*, 646, 36–49.
- Moskowitz, B. M. (1981). Methods for estimating Curie temperatures of titanomagnetites from experimental J_s -T data. *Earth and Planetary Science Letters*, 53, 84–88.
- Panaiotu, C. G., Panaiotu, C. E., & Lazar, I. (2012). Remagnetization of Upper Jurassic limestones from the Danubian Unit (Southern Carpathians, Romania): Tectonic implications. *Geologica Carpathica*, 63(6), 453–461.
- Pavlović, Z., Marković, B., Atin, B., Dolić, B., Gagić, N., Marković, O., et al. (1979). *Basic Geological Map of SFRJ, sheet Smederevo (scale 1:100 000)*. Beograd: Savezni Geološki Zavod.
- Prelević, D., Cvetković, V., Jovanović, M. (2000). The composite dome of Beli Kamen (Mt. Rudnik, Central Serbia) – the example of a specific interaction of lamprophyric and granitoid magma. In S. Karamata & S. Janković (Eds.), *Geology and Metallogeny of the Dinarides and the Vardar zone*, (pp. 255–267). The Academy of Sciences and Arts of the Republic of Srpska, Collections and Monographs, Book 1, Department of Nature, Mathematical and Technical Science.
- Prelević, D., Foley, S. F., Romer, R. L., & Cvetković, V. (2005). Tertiary Ultrapotassic Volcanism in Serbia: Constrains on Petrogenesis and Mantle Source Characteristics. *Journal of Petrology*, 46(7), 1443–1487.
- Schefer, S., Cvetković, V., Fügenschuh, B., Kounov, A., Ovtcharova, M., Schaltegger, U., et al. (2011). Cenozoic granitoids in the Dinarides of Southern Serbia: Age of intrusion, isotope geochemistry, exhumation history and the significance for the geodynamic evolution of the Balkan Peninsula. *International Journal of Earth Science*, 100, 1181–1206.

- Schmid, S. M., Bernoulli, D., Fügenschuh, B., Matenco, B., Schefer, S., Schuster, R., et al. (2008). The Alpine – Carpathian – Dinaric orogenic system: Correlation and evolution of tectonic units. *Swiss Journal of Geoscience*, *101*, 139–183.
- Thébaud, E., Finlay, C. C., Beggan, C. D., Alken, P., Aubert, J., Barrois, O., et al. (2015). International Geomagnetic Reference Field: The 12th generation. *Earth, Planets and Space*. <https://doi.org/10.1186/s40623-015-0228-9>.
- Toljić, M., Matenco, L., Ducea, M. N., Stojadinović, U., Milivojević, J., & Đerić, N. (2012). The evolution of a key segment in the Europe-Adria collision: The Fruška Gora of northern Serbia. *Global and Planetary Change*, *103*, 39–62.
- Toljić, M., Matenco, L., Stojadinović, U., Willinshofer, E., & Ljubović-Obradović, D. (2018). Understanding fossil fore-arc basins: Inferences from the Cretaceous Adria-Europe convergence in the NE Dinarides. *Global and Planetary Change*. <https://doi.org/10.1016/j.gloplacha.2018.01.018>.
- Torsvik, T. H., Van der Voo, R., Preeden, U., Mac Niocaill, C., Steinberger, B., Doubrovine, P. V., et al. (2012). Phanerozoic polar wander, paleogeography and dynamics. *Earth-Science Reviews*, *114*, 325–368.
- Urošević, M., Pavlović, Z., Klisić, M., Brković, T., Malšević, M., Stefanović, M., et al. (1973a). *Geological map and Explanatory Notes of the Basic Geological Map of SFRJ, sheet Vrnjci (1:100 000)* (p. 69). Beograd: Savezni Geološki Zavod.
- Urošević, M., Pavlović, Z., Klisić, M., Karamata, S., Brković, T., Malšević, M., et al. (1973b). *Geological map and Explanatory Notes of the Basic Geological Map of SFRJ, sheet Novi Pazar (1:100 000)* (p. 77). Beograd: Savezni Geološki Zavod.
- Ustaszewski, K., Schmid, S., Fügenschuh, B., Tischler, M., Kissling, E., & Spakman, W. (2008). A map-view restoration of the Alpine – Carpathian – Dinaric system for the Early Miocene. *Swiss Journal of Geoscience*, *101*(suppl. 1), 273–294.
- van Hinsbergen, D. J. J., Dupont-Nivet, G., Nakov, R., Oud, K., & Panaiotu, C. (2008). No significant post-Eocene rotation of the Moesian Platform and Rhodope (Bulgaria): Implication for the kinematic evolution of the Carpathian and Aegean arcs. *Earth and Planetary Science Letters*, *273*, 345–358.
- van Hinsbergen, D. J. J., Mensink, M., Langereis, C. G., Maffione, M., Spalluto, L., Tropeano, M., et al. (2014). Did Adria rotate relative to Africa? *Solid Earth*, *5*, 611–629.
- Wilson, R.L., Dagley, P., McCormack, A.G. (1972). Paleomagnetic evidence about the source of the geomagnetic field. *Geophysical JR. Astron Soc*, *28*, 213–224.